Geophysical Research Letters

RESEARCH LETTER
10.1029/2022GL101775

Freshwater Transport Over the Northeast Greenland Shelf in Fram Strait

T. Karpouzoglou[1,2], L. de Steur[1], and P. A. Dodd[1]

[1]Norwegian Polar Institute, Tromsø, Norway, [2]Geophysical Institute, University of Bergen, Bergen, Norway

Key Points:

- Summer freshwater transport (FWT) over the shelf cumulates to −27 mSv and shows no trend in time
- New mooring data on the shelf at 10.1°W show a very large seasonal cycle
- Year-round FWT over the shelf is estimated to ∼−52 mSv or 43% of the total freshwater outflow from the Fram Strait

Supporting Information:

Supporting Information may be found in the online version of this article.

Correspondence to:

T. Karpouzoglou,
thodoris.karpouzoglou@npolar.no

Citation:

Karpouzoglou, T., de Steur, L., & Dodd, P. A. (2023). Freshwater transport over the Northeast Greenland shelf in Fram Strait. *Geophysical Research Letters*, *50*, e2022GL101775. https://doi.org/10.1029/2022GL101775

Received 20 OCT 2022
Accepted 30 DEC 2022

Author Contributions:

Conceptualization: T. Karpouzoglou, L. de Steur
Formal analysis: T. Karpouzoglou
Funding acquisition: L. de Steur
Investigation: T. Karpouzoglou
Methodology: T. Karpouzoglou, L. de Steur, P. A. Dodd
Project Administration: L. de Steur
Resources: L. de Steur
Supervision: L. de Steur, P. A. Dodd
Visualization: T. Karpouzoglou
Writing – original draft: T. Karpouzoglou
Writing – review & editing: L. de Steur, P. A. Dodd

Abstract We assess the contribution of flow over the Northeast Greenland Shelf (NEGS) to the total freshwater transport (FWT) through the Fram Strait. We analyze available observations since 2013 consisting of hydrographic sections, new mooring data, and surface-geostrophic velocity and ERA5 winds. We provide first seasonal estimates of the FWT over the entire shelf and find a net southward FWT between 47 and 56 mSv (reference salinity 34.9), or ∼40%–45% of the total FWT through the Fram Strait. In summer, the long-term mean FWT east of 8°W cumulates to 27 mSv southward, there is no trend toward increasing FWT, and new mooring data show a large seasonal cycle. We show that the NEGS contributes significantly to the Arctic freshwater outflow, however, uncertainty is high. To close the Arctic freshwater budget and provide better FWT estimates to the North Atlantic, sustained year-round observations on the NEGS are essential.

Plain Language Summary We use new observations since 2013 to calculate transport over the Northeaster Greenland Shelf for the first time, and investigate how much it adds to the transport of the East Greenland Current over the shelf break which is monitored by moorings. Over most of the shelf, direct observations of ocean properties are limited to summer. Thus, we use remote-sensing and wind reanalysis data, with shelf-wide and year-round coverage, but higher uncertainty, to estimate the year-round transport of low-salinity water (freshwater, less than 34.9) over the entire shelf. We find that on the shelf, freshwater transport is at least 40% of the total in Fram Strait. Still, uncertainty is high and year-round, direct observations in the western part of the shelf are required to provide accurate estimates for the Arctic freshwater outflow.

1. Introduction

In a period of Arctic Ocean freshening, accurate monitoring of the Arctic outflow is essential as it supplies southern latitudes with fresh water that participates in the overturning circulation and may modulate dense water formation (Le Bras et al., 2021; Stommel, 1961). Since 1997, the shelf-break East Greenland Current (EGC), which transports liquid fresh water and sea-ice southward, has been monitored in the Fram Strait by moorings between 6.5° and 2°W (De Steur et al., 2009; Fahrbach et al., 2001). In 2003, the array was extended to 8°W on the shelf, increasing the captured freshwater transport (FWT) significantly (De Steur et al., 2018) and in the period 2003–2019 the average liquid FWT between 8° and 2°W was −69.1 ± 9.4 mSv (reference salinity 34.9, Karpouzoglou et al. (2022)). However, the transport over the ∼200 km wide Northeast Greenland Shelf (NEGS) west of 8°W is poorly known leaving a large uncertainty in the total FWT from the area. Motivated by recent studies suggesting a coastal current (surface water jet) flowing along the East Greenland shelf (Foukal et al., 2020; Håvik et al., 2017), and from the need for a closed Arctic freshwater budget (Tsubouchi et al., 2018), we investigate the contribution of the NEGS to the total liquid FWT to southern latitudes.

The NEGS is ice-covered during most of the year inhibiting in situ observations. Early analyses of summer hydrographic observations (Bourke et al., 1987; Budéus & Schneider, 1995; Budéus et al., 1997) suggest an anticyclonic circulation following the local trough system with the northward flowing limb, referred to as East Greenland Coastal Counter Current (EGCCC), adjacent to the Greenland coast (Figure 1b). Winter circulation, however, is less known. Based on mooring measurements (1992–1993) in the Westwind trough Topp & Johnson (1997) find that in winter, when the area is ice-covered and the sea-surface is shielded from the wind, the EGCCC intensifies, variability decreases and the observed flow (deeper than 75 m) aligns with the bathymetry implying that the flow is topographically steered. Recently, mooring observations (2014–2016) in the Norske trough (Münchow et al., 2020) show that the near-surface flow is northward only in summer and reverses in winter, suggesting that a near-surface anticyclonic circulation in the NEGS might only be a seasonal feature.

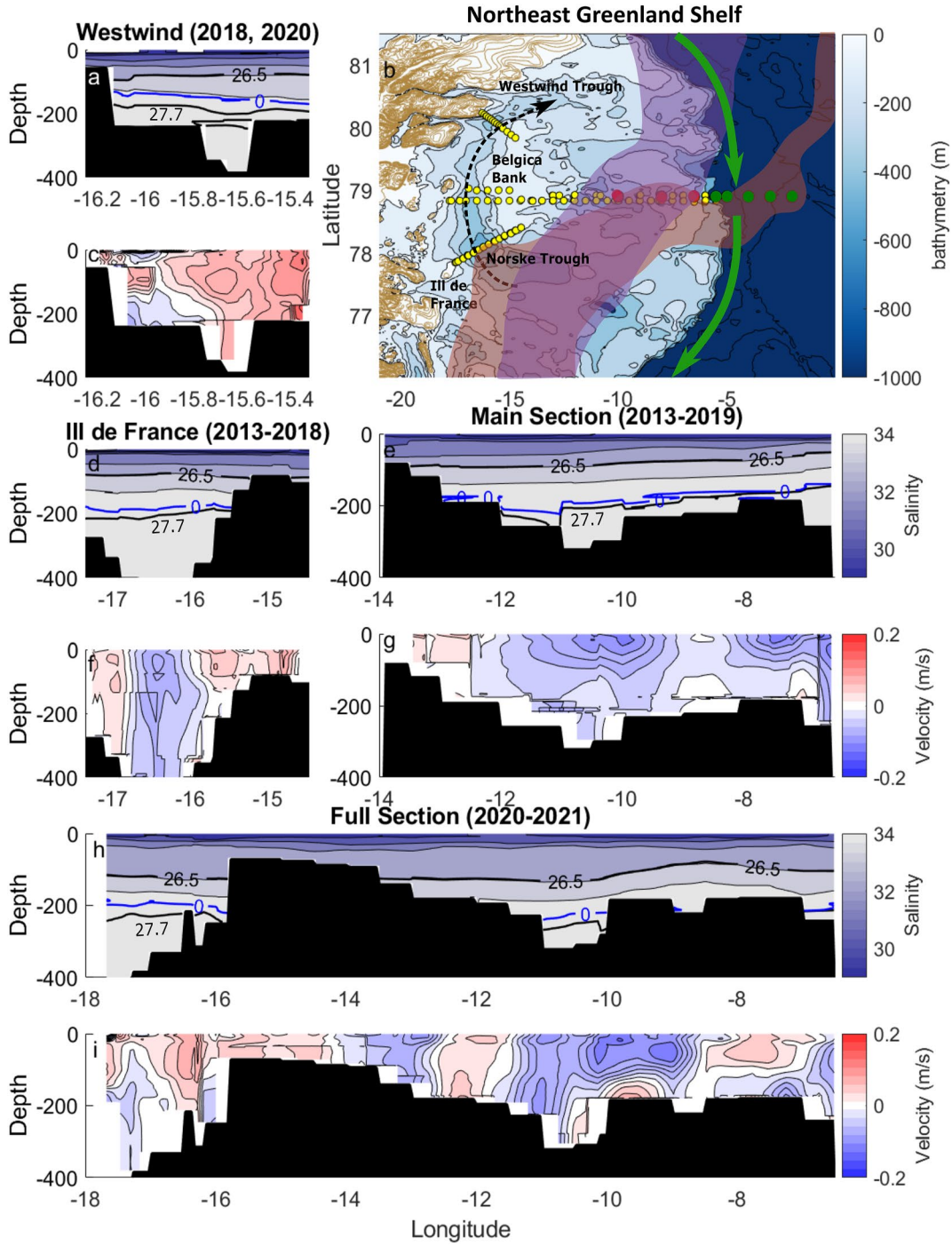

Figure 1. Mean salinity (a, d, e, h) and absolute geostrophic velocity from the CTD referenced to the VMADCP (c, f, g, i). The contours show the isopycnals $\sigma_\theta = 26.5$ kg/m^3 and $\sigma_\theta = 27.7$ kg/m^3 (black), and the isotherm $T = 0$°C (blue). (b) Map of the NEGS. The dots show the position of CTD casts at the Westwind, IdF, and Main (78.9°N) sections (yellow) and the positions of the moorings on the NEGS: F20, F17, and F14, at 10.1°, 8°, and 6.5°W (red). The moorings over the shelf-break EGC are shown in green. The arrows show the anticyclonic circulation suggested by Budéus and Schneider (1995) with the EGCCC adjacent to the Greenland coast (black dashed) and the EGC at the shelf-break (green). The envelopes show suggested surface pathways of PW over the shelf in winter/autumn 2015 (purple) and summer 2020 (red) obtained from IABP buoys (see Section 2.3).

The anticyclonic circulation over the NEGS suggests that any estimate of the southward transport through Fram Strait is sensitive to the zonal extent of the area of integration (De Steur et al., 2009). Until recently, due to the dense ice coverage only few sections have extended to the Greenland coast, and only in summer. Based on one such section in 2005, Rabe et al. (2013) find that FWT in summer cumulates to zero west of 10.6°W. Moreover, using six hydrographic sections between 1998 and 2011 they calculated the FWT east of 10.6°W and up to 6.5°W they found it to cumulate to ∼−50 mSv, about 50% of the total transport in Fram Strait. De Steur et al. (2009) used a coarse-resolution ice-ocean-model simulation to estimate the seasonality of the flow over the shelf and they found minimum transport in early summer and maximum in late fall. The modeled annual mean FWT west of 6.6°W was estimated at −25.6 ± 11.3 mSv, that is, 55% of the total FWT in the Fram Strait.

To estimate the FWT west of 8°W, not captured by the mooring array, we use new mooring data and hydrographic sections over the NEGS since 2013, combined with vessel-mounted acoustic Doppler profiler measurements (VMADCP). To calculate the summer FWT we use two new hydrographic sections reaching the Greenland coast (2020, 2021) and combine earlier ones across the eastern shelf and the Norske trough, to create a full section spanning from the Greenland coast to the shelf break (Figure 1). Additionally, a new mooring allows extension of the year-round transport estimate to 10.1°W. Finally, based on surface velocity from absolute dynamic topography (ADT) and wind velocity (ERA5) we analyze the seasonality, show that winter FWT is significantly larger than in summer, and provide first estimates of year-round FWT over the entire NEGS.

2. Data and Methods

2.1. Summer Shipboard Data

We analyze data collected over the NEGS (west of 6.5°W) from eight summer (July to September) cruises since 2013 (see Text S4 in Supporting Information S1). Hydrographic data were acquired on three sections across the NEGS, namely the Main section at 78.9°N, the Île de France (IdF) section crossing the Norske trough in the south, and the Westwind section crossing the Westwind trough in the north (Figure 1b). Between 2013 and 2018, the Main section extended westward to the land-fast ice at Belgica Bank (13°–14°W) (Figures 1e and 1g) and was complemented by the IdF section (14.5°–18°W) (Figures 1d and 1f). In 2020 and 2021, due to a complete breakup of the land-fast ice (De Steur, 2022), the Main section extended to the Greenland coast (Figures 1h and 1i). Data from the Westwind section are only available for 2018 and 2020 (Figures 1a and 1c).

We use thermal wind balance to calculate the geostrophic velocity and reference it to the VMADCP velocity averaged between 50 and 100 m. To calculate the FWT to the Greenland coast, we combine the IdF and Main sections to the so-called Full section neglecting small latitudinal differences, grid the data with 1 km horizontal resolution and average over the 8 years. In different years the Main and IdF sections had different westward extensions (Figure 2b). Thus, before integrating across the shelf we fill data gaps with the long-term mean. Then, FWT is calculated as:

$$FWT = \int\int V_{(x,z)} \frac{S_r - S_{(x,z)}}{S_r} dz dx, \quad (1)$$

where $V_{(x,z)}$ and $S_{(x,z)}$ are the absolute geostrophic velocity and salinity, while reference salinity S_r is set to 34.9, the mean salinity of the Nordic Seas (Holfort & Meincke, 2005). We address concerns about the use of the reference salinity (Bacon et al., 2015; Schauer & Losch, 2019) in Section S5 in Supporting Information S1. We integrate over the Polar Water (PW) defined as the water with potential density anomaly $\sigma_\theta < 27.7$ kg/m^3 (Rudels et al., 2005) and along the Full section between 6.5°W and the Greenland coast.

2.2. Mooring Data

We use hydrographic and velocity data between September 2020 and July 2021 from three moorings on the NEGS, namely from F14 and F17 deployed at 6.5°W and 8°W, and from a new mooring F20, deployed at 10.1°W for the first time in 2020 (see Text S4 in Supporting Information S1). Time series of F14 and F17 between 2013 and 2019 are used for comparison (Karpouzoglou et al., 2022).

2.3. Additional Data Products and Seasonal Estimates

We provide two estimates of seasonality and year-round FWT west of 8°W. First, we analyze two CTD sections from spring (April to June) cruises in 2008 and 2018 providing salinity temperature and geostrophic velocity

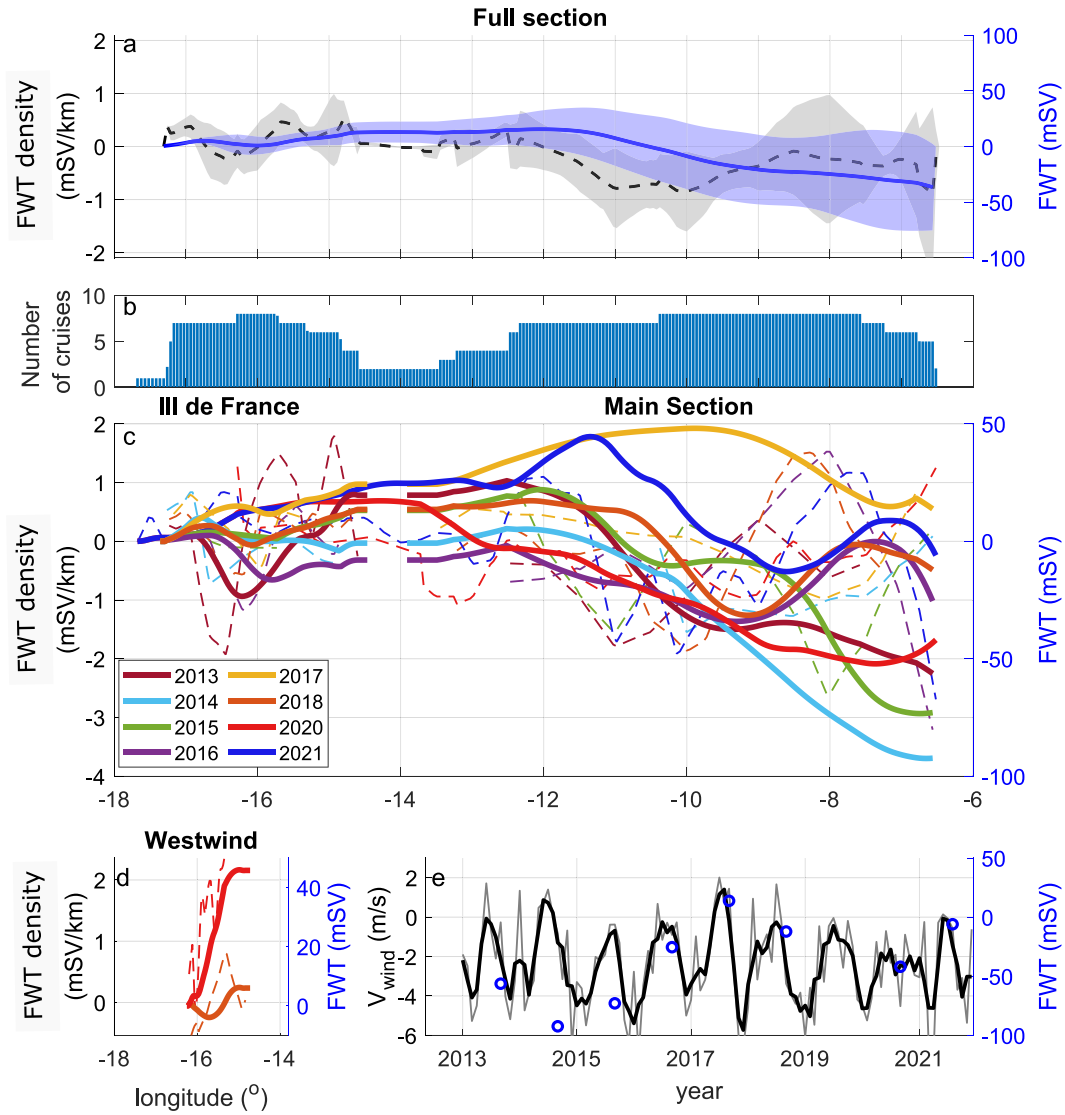

Figure 2. (a) Summer-mean meridional FWT density and cumulative FWT from the CTD data across the Full section. Shaded areas show the 1 std from the mean. (b) Cruise number per longitude. (c) Meridional FWT density and cumulative FWT from the individual years in the Full section and (d) Westwind section. (e) Monthly-mean (gray) and 3 month smoothed meridional wind velocity (black lines) averaged over the NEGS (20°–0°W and 76°–82°N) compared with the FWT integrated over the Full section for the individual years (blue circles).

up to 9.5°W. From those, we calculate the mean spring section and extended it to the Greenland coast through regression with the summer mean section (see Text S6, Figure S1 left in Supporting Information S1). Then, the mean summer and spring sections are cubically interpolated in time to obtain 3-month seasonal climatologies of geostrophic velocity and salinity (Figure S1 right in Supporting Information S1). Geostrophic velocity at 8° and 10.1°W is referenced to the depth-averaged velocity from the moorings and is interpolate linearly between 11.5° and 8°W. West of 11.5°W where there are no moorings and flow is mostly barotropic, we reference at the surface with a 3-month climatology of surface velocity obtained from two ADT datasets (Andersen & Knudsen, 2009; Müller et al., 2019; Rose et al., 2019a) (see Text S1 in Supporting Information S1).

Additionally, we use monthly-mean 10 m meridional winds from ERA5 (Hersbach et al., 2020) averaged over the NEGS (20°–0°W and 76°–82°N) to investigate seasonal variability and to obtain a proxy of the volume transport (VT) and FWT over the NEGS. Finally, we use buoy trajectories from the International Arctic Buoy Program (IABP) (Rigor et al., 2002) as a first-order indication of the pathways of the PW onto the NEGS (Figure 1b). We show buoy trajectories that entered the shelf and crossed 77°N west of 10°W, and distinguish two groups arriving

Table 1
(a) Observations and Year-Round Estimates of FWT (mSv) From Different Longitudinal Sections and Different Datasets

West of:	16°W	11.5°W	10.1°W	8°W	6.5°W
$CTD^{summer}_{2013-21}$	+1 ± 9	+11 ± 20	−12 ± 29	−27 ± 33	−39 ± 41
$CTD^{summer}_{2020-21}$	+13	+18	−5	−27	−23
Estimate I	–	–	–	−47.1 ± 30	–
Estimate II	−13 ± 12	−10 ± 14	−29 ± 19	−56 ± 26	–
Between:				10.1°W–8°W	8°W–6.5°W
$Moorings_{2013-2019}$	–	–	–	–	−23 ± 2.5
$Moorings_{2020-2021}$	–	–	–	−13.6	−22.3
$CTD^{summer}_{2013-21}$	–	–	–	−16.1 ± 4	−11.9 ± 7.4

at 78.9°N in summer (July–September) 2020, and winter and autumn (January–March, October–December) 2015 (see Text S2 in Supporting Information S1).

3. Results

3.1. Summer Transport

The mean summer FWT in 2013–2021 cumulates to zero west of 10.7°W, in agreement with the results from Rabe et al. (2013), while between 10.7°W and 6.5°W it cumulates to a southward flow of 39 mSv (±41 mSv standard deviation, Figure 2a, Table 1). Of this, 27 ± 33 mSv occur west of 8°W and are thus not captured by the mooring-based estimate from Karpouzoglou et al. (2022). FWT from the shipboard data shows large interannual variability (Figures 2c and 2d). A sensitivity experiment where salinity from the individual years is exchanged with the long-term mean (not presented) shows that cumulated FWT does not depend significantly on the summer-to-summer variations in salinity but that the interannual variability of FWT is primarily due to velocity.

The FWT varies longitudinally; west of 14°W FWT is mainly northward (Figures 2c and 2d) associated with the EGCCC (Figures 1c, 1f, and 1i) but it is southward further east. Between 11.5° and 9.5°W, a southward surface intensified current followed the local topography, while centered at 8°W we observe a current with variable direction from southward (2013–2015, 2017, 2020) to northward (2016, 2018, 2021, Figure 2c). The weakening or even reversal of this current core after 2015 was partly responsible for the decreased FWT in the shelf-break EGC (8°–2°W) presented by Karpouzoglou et al. (2022). Here we show that after 2015 summer FWT decreased as well over the NEGS west of 8°W (Figure 2e, blue circles), suggesting that since 2015 less fresh water is flowing from Fram Strait to southern latitudes.

3.2. Year-Round Transport (2020–2021)

Between September 2020 and July 2021, the FWT obtained from the moorings between 10.1° and 6.5°W showed a large seasonal cycle, ranging from −13.4 mSv in summer to −66.4 mSv in winter (January to March) with a one-year average of −35.9 mSv (Figure 3a). Of that, −13.6 mSv occurred between 10.1° and 8°W, while the CTD derived estimate in the same area for summer is −16.1 mSv (Figure 3a blue dot, Table 1). However, during this time period wind speed often exceeded one standard deviation from the 2013–2021 mean (Figure 3d), and so did FWT, VT and freshwater content (FWC) east of 8°W (Figures 3a–3c). In March-April 2020, the southward FWT and VT east of 8°W were exceptionally large due to concurring large southward wind velocity, however, in October, November, and May, VT west of 8°W was northward while wind was weaker than normal (Figures 3b and 3d). We hypothesize that during these months, the northward FWT west of 8°W was also anomalous and related to the weak northerlies, and thus the estimated FWT between 10.1° and 8°W for 2020–2021 likely underestimates the long-term mean value.

3.3. Estimates of Seasonality

Both southward wind and FWT from the moorings in 2020–2021 were larger in winter (December to March) than in summer (Figures 3a and 3d), suggesting that the seasonally varying FWT is driven by seasonal winds which induce a sea-level gradient across the strait and drive geostrophic currents (Armitage et al., 2018). First,

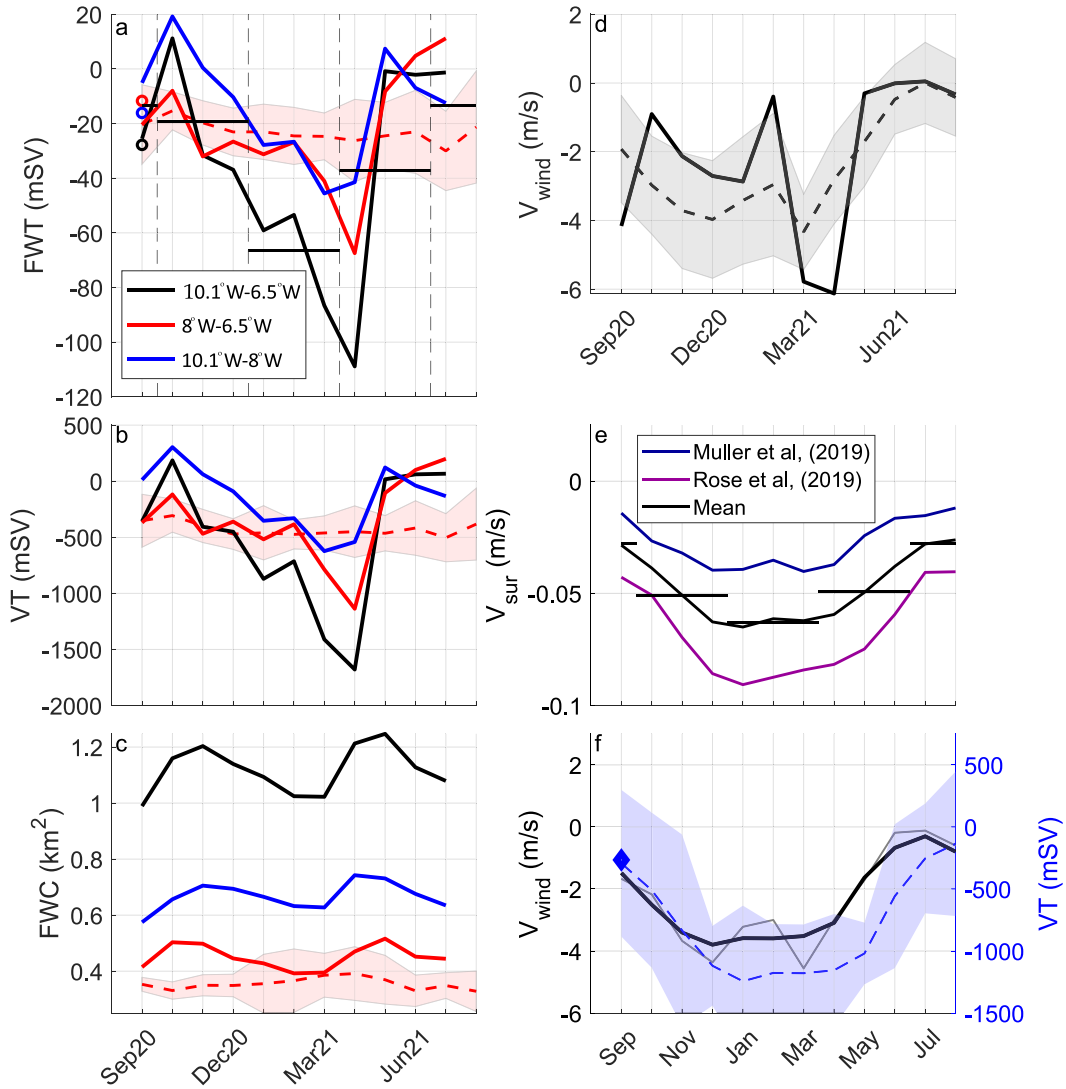

Figure 3. September 2020 to July 2021 (a) FWT, (b) VT, and (c) FWC from the shelf moorings between 10.1° and 6.5°W (black), 8°–6.5°W (red), and 10.1°–8°W (blue). The dashed lines shows the 2013–2019 means between 8° and 6.5°W. The dots in panel (a) show the mean FWT from the summer CTD data. (d) Meridional wind velocity from the ERA5 data averaged over the NEGS (solid line) and the 2013–2019 mean (dashed). Monthly climatology of (e) meridional surface velocity averaged over the Full section from the ADT datasets of Müller et al. (2019) (2008–2012) and Rose et al. (2019a) (2013–2018), and their mean. (f) Monthly (gray) and 3-month smoothed (black) meridional wind climatology, and September mean VT from the CTD cumulated from the Greenland coast to 8°W (blue diamond). The dashed line shows the linearly regressed seasonal estimate of VT. The envelopes show the one standard deviation from the mean.

we provide estimate I of the seasonality of FWT using wind as a proxy. Except for 2014 and 2015 when the high FWT and VT correspond to low wind velocity (Figure 2e, Figure S4 in Supporting Information S1), there is good, significant, correlation ($R = 0.97$) between August meridional wind and the ship-based estimates of VT, usually in September. A linear fit of VT in the PW cumulated to 8°W as a function of wind velocity averaged over the NEGS shows that VT = 317 × V_{wind} − 40 [mSv] (Figure S4 in Supporting Information S1). Assuming that this 1-month lagged relationship holds throughout the year, we calculate the VT from the smoothed wind climatology (Figure 3f) and multiply it with the FWC climatology (Figure S1 in Supporting Information S1) to obtain FWT. We find it to range between −70 ± 39 mSv in winter (January to March) and −15 ± 24 mSv in summer (Figure 4d), while the year-round FWT west of 8°W is −47 ± 30 mSv (Table 1).

Salinity and southward geostrophic velocity from the CTD climatologies show a maximum in winter/spring and minimum in summer (Figure S1 in Supporting Information S1). Velocity from both ADT products show similar

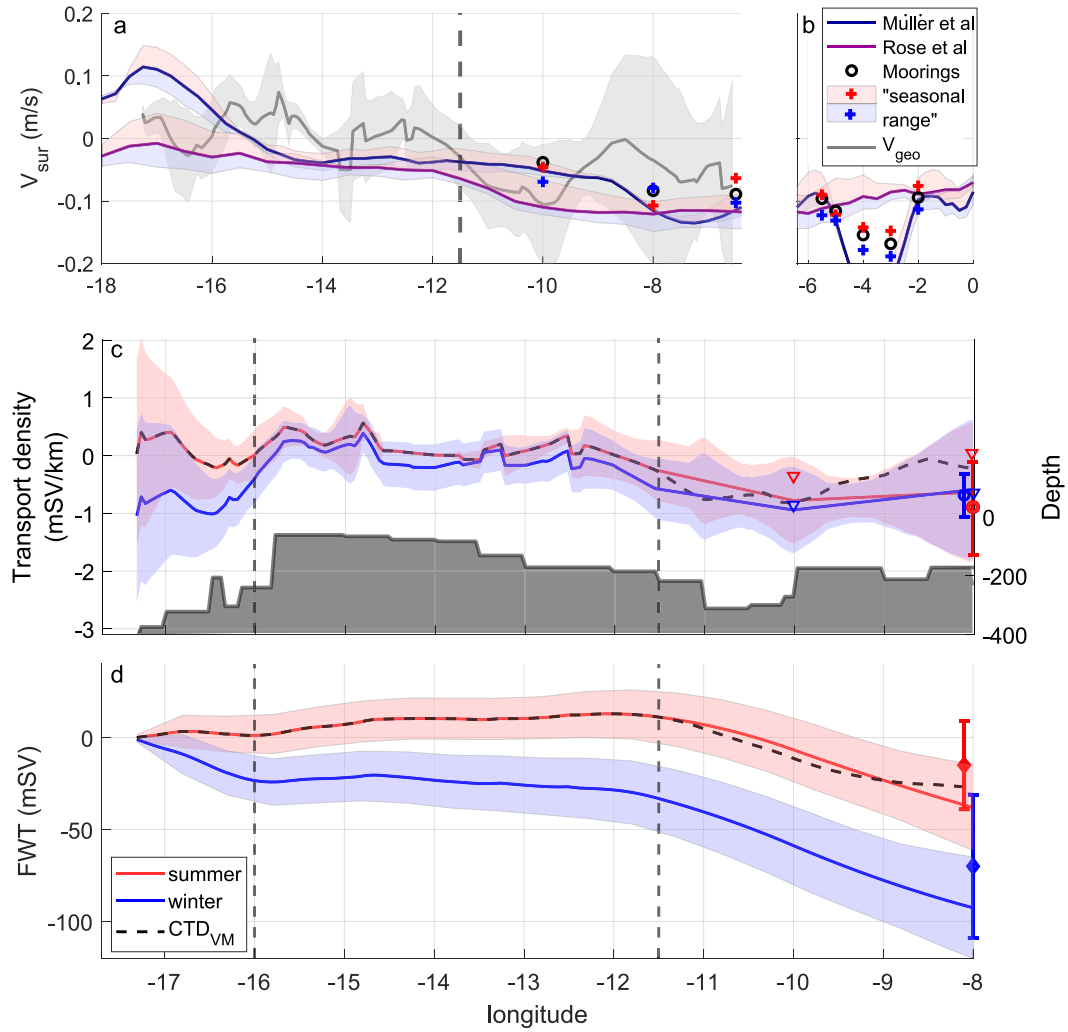

Figure 4. (a, b) Surface current velocity derived from the ADT data from Müller et al. (2019) (blue) and Rose et al. (2019a) (purple). Together we present the top 50 m velocity from the moorings (black dots) and the CTDs referenced to the VMADCP (gray, shading: ±1 std). Colored shading and crosses show the seasonal range between summer (July–September: red) and winter (January–March: blue). (c) Summer and winter FWT density along the full section. The FWT density at the two mooring locations between 2020–2021 (triangles) and 2013–2019 (circles) are also shown. (d) Cumulative FWT, the envelopes indicate the uncertainty taking into account the random occurrence of the error. The red and blue diamonds show the summer and winter FWT calculated from the wind-derived estimate I with the standard deviation as error bars.

seasonality with stronger southward velocity in winter than in summer, however, the mean values of the two ADT datasets over the section differ by 4 cm/s (Figure 3e). West of 15°W the difference exceeds 10 cm/s, there the product of Müller et al. (2019) shows a strong northward velocity corresponding to the EGCCC persisting year-round, while the product of Rose et al. (2019a) shows general southward velocity that only becomes northward in summer (Figure 4a). Between 15°W and 11.5°W, both products show weak southward velocity year-round.

For estimate II, we calculate the mean surface velocity by averaging the two products and calculate a 3-month seasonal climatology (Figure 3e) to which we reference the geostrophic velocity west of 11.5°W (Figure S1 in Supporting Information S1, Section 2.3), and correct for the difference between the summer values and the observations presented in Section 3.1 (Figure 4c). Then we calculate the FWT density for all seasons. Up to 8°W, FWT cumulates to −38 ± 25 mSv in summer and −92 ± 26 mSv in winter (Figure 4d) with the mean at −56 ± 26 mSv (Table 1, see Text S3 in Supporting Information S1 for the calculation of uncertainty).

4. Discussion

The EGCCC (west of 16°W) flows northward in summer (Budéus & Schneider, 1995; Budéus et al., 1997), however in our estimate II it reverses southward in winter (Figure 4c). This relates to the small mean FWT in the EGCCC from the summer 2013–2021 CTD data, which is largely due to the IdF sections, as the 2020–2021 full sections showed a stronger EGCCC (Table 1). Nevertheless, this reversal agrees with the seasonality of surface velocity from the product of Rose et al. (2019a) (Figure 4a) and with the near-surface mooring observations from Münchow et al. (2020), however, it disagrees with the product of Müller et al. (2019) and the mooring observations from Topp & Johnson (1997) which showed that the EGCCC flows northward year-round. The EGCCC accounts for 23% of the year-round FWT (Table 1), as there is no further evidence for its southward reversal in winter, our estimate II is possibly too high. The same holds for estimate I which assumes that the derived relationship between wind and VT for summer also holds in winter, when the shelf freezes up and the ice is grounded to the shallow Belgica Bank and the Greenland coast. As land-fast ice shields ocean surface from the wind, the same wind velocity in winter likely drives smaller VT.

From two groups of IABP buoys arriving at Fram Strait in 2020 (summer) and 2015 (winter/autumn) 40% crossed 78.9°N west of 8°W (weighted average relative to the number of buoys per group, see Text S2 in Supporting Information S1), which is in agreement with the estimates from Section 3.3. Moreover, we find that buoy trajectories remain east of Belgica Bank (13°W) in winter/autumn 2015 and east of 10°W in summer 2020 (Figure 1b). Even though this may be related to the initial position of each buoy deployment (Figure S3 in Supporting Information S1), it also suggests that the point of zero cumulated FWT found at 10.7°W in summer (Section 3.1) moves west in winter. Such a seasonal change could be explained by stronger northerly winds in autumn/winter and the corresponding Ekman transport, strengthening and shifting the PW pathways in winter further onto the shelf (Håvik & Våge, 2018). The few buoys furthest west freeze in winter and cannot provide information on the winter circulation of the EGCCC.

5. Conclusions

We have analyzed summer hydrographic sections, new mooring data, surface current velocity from ADT, and wind velocity reanalysis from the NEGC and provide first year-round estimates of FWT west of 8°W. We find that FWT ranges from −47 to −56 mSv. Provided a mean FWT between 8° and 2°W of −69.1 ± 9.4 mSv (Karpouzoglou et al., 2022), our estimate of FWT on the NEGS west of 8°W is 40%–45% of the total FWT through the Fram Strait. Additionally, hydrographic observations show that summer FWT is −27 mSv west of 8°W and shows no increasing trend since 2013, while it cumulates to zero west of 10.7°W. One year of mooring data (September 2020–July 2021) shows a large seasonal cycle, however, a small year-round contribution of −13.6 mSv between 8° and 10.1°W, likely since local winds were weaker throughout most of this year.

We showed that the NEGS contributes significantly to the Arctic freshwater outflow, adding nearly half of the total FWT occurring in Fram Strait, however, due to the absence of year-round observations on the western shelf, estimates are still subject to high uncertainty. The near-surface seasonality in the EGCCC is key for determining the total FWT over the NEGS and direct year-round observations are essential for improving the current estimates. Mooring deployments in the Norske Trough may provide valuable information, not only for the pathways of Atlantic Water toward Greenland (Münchow et al., 2020; Schaffer et al., 2017), but also for the near-surface seasonality of the EGCCC and hence the total FWT over the NEGS.

Conflict of Interest

The authors declare no conflicts of interest relevant to this study.

Data Availability Statement

The CTD cast data from the different cruises became available from: Dodd, Almgren, et al. (2022), Dodd, Aloise, et al. (2022), Dodd, Anhaus, et al. (2022), Dodd, Ask, et al. (2022), Dodd, Chierici, et al. (2022), Dodd, Debyser, et al. (2022), Dodd, Divine, et al. (2022), Dodd, Gonçalves-Araujo, et al. (2022). The mooring data have been available from de Steur (2021) and Karpouzoglou & de Steur (2021). One of the datasets of absolute dynamic

topography is available by Müller et al. (2019). The other have been calculated from sea surface height from Rose et al. (2019b) and mean dynamic topography downloaded from: https://ftp.spacecenter.dk/pub/DTU19/MDT/.

Acknowledgments
The authors thank Benjamin Rabe and the one anonymous reviewer for their constructive comments that helped in improving this paper. This work was carried out from the FreshArc project supported by the Norwegian Research Council through the FRIPRO program (Grant 286971). Furthermore, the authors like to thank Kristen Fossan for servicing the moorings and instruments and thanks to all crew of R/V Lance and R/V Kronprins Haakon.

References

Andersen, O. B., & Knudsen, P. (2009). DNSC08 mean sea surface and mean dynamic topography models. *Journal of Geophysical Research*, *114*(C11), C11001. https://doi.org/10.1029/2008JC005179

Armitage, T. W. K., Bacon, S., & Kwok, R. (2018). Arctic sea level and surface circulation response to the arctic oscillation. *Geophysical Research Letters*, *45*(13), 6576–6584. https://doi.org/10.1029/2018GL078386

Bacon, S., Aksenov, Y., Fawcett, S., & Madec, G. (2015). Arctic mass, freshwater and heat fluxes: Methods and modelled seasonal variability. *Philosophical Transactions of the Royal Society A: Mathematical, Physical & Engineering Sciences*, *373*(2052), 20140169. https://doi.org/10.1098/rsta.2014.0169

Bourke, R. H., Newton, J. L., Paquette, R. G., & Tunnicliffe, M. D. (1987). Circulation and water masses of the East Greenland shelf. *Journal of Geophysical Research*, *92*(C7), 6729–6740. https://doi.org/10.1029/JC092iC07p06729

Budéus, G., & Schneider, W. (1995). On the hydrography of the Northeast water polynya. *Journal of Geophysical Research*, *100*(C3), 4287–4299. https://doi.org/10.1029/94JC02024

Budéus, G., Schneider, W., & Kattner, G. (1997). Distribution and exchange of water masses in the Northeast Water polynya (Greenland Sea). *Journal of Marine Systems*, *10*(1), 123–138. https://doi.org/10.1016/S0924-7963(96)00074-7

de Steur, L. (2021). *Moored current meter and hydrographic data from the Fram strait arctic outflow observatory since 2009*. Norwegian Polar Institute. https://doi.org/10.21334/npolar.2021.c4d80b64

De Steur, L. (2022). Fram strait cruise repot, 31 July–20 August 2021: Cruise no. 2021709.

De Steur, L., Hansen, E., Gerdes, R., Karcher, M., Fahrbach, E., & Holfort, J. (2009). Freshwater fluxes in the East Greenland current: A decade of observations. *Geophysical Research Letters*, *36*(23), L23611. https://doi.org/10.1029/2009GL041278

De Steur, L., Peralta-Ferriz, C., & Pavlova, O. (2018). Freshwater export in the East Greenland current freshens the North Atlantic. *Geophysical Research Letters*, *45*(24), 13359–13366. https://doi.org/10.1029/2018GL080207

Dodd, P. A., Almgren, P. A., Blæsterdalen, T., Debyser, M., Guthrie, J., Granskog, M. A., et al. (2022). *CTD profiles from NPI cruise FS2017 to the FRAM strait including auxiliary sensors*. Norwegian Polar Institute. https://doi.org/10.21334/npolar.2022.44db5c55

Dodd, P. A., Aloise, A., Cooper, A., Ghani, M., Johansson, A. M., Kalhagen, K., et al. (2022). *CTD profiles from NPI cruise FS2015 to the Fram strait including auxiliary sensors*. Norwegian Polar Institute. Retrieved from https://data.npolar.no/dataset/52ecdc98-3fbd-46a2-8f08-1ac5d923da14

Dodd, P. A., Anhaus, P., Chierici, M., Doncila, A., Fransson, A., Granskog, M. A., et al. (2022). *CTD profiles from NPI cruise FS2016 to the Fram strait including auxiliary sensors*. Norwegian Polar Institute. https://doi.org/10.21334/npolar.2022.29c6e2c7

Dodd, P. A., Ask, A., Divine, D., Granskog, M. A., Keck, A., Kern, Y., et al. (2022). *CTD profiles from NPI cruise FS2020 to the Fram strait including auxiliary sensors*. Norwegian Polar Institute. Retrieved from https://data.npolar.no/dataset/5df344c6-2ae8-432c-ad54-5c2e918b77df

Dodd, P. A., Chierici, M., Debyser, M., Fransson, A., Granskog, M. A., Hamar, A. L., et al. (2022). *CTD profiles from NPI cruise FS2018 to the Fram strait including auxiliary sensors*. Norwegian Polar Institute. https://doi.org/10.21334/npolar.2022.2c646c2e

Dodd, P. A., Debyser, M., Desmet, F., Gonçalves-Araujo, R., Granskog, M. A., Karpouzoglou, T., et al. (2022). *CTD profiles from NPI cruise FS2019 to the Fram strait including auxiliary sensors*. Norwegian Polar Institute. https://doi.org/10.21334/npolar.2022.5066a075

Dodd, P. A., Divine, D., Granskog, M. A., Johansson, A. M., Kern, Y., Pavlov, A. K., et al. (2022). *CTD profiles from NPI cruise FS2014 to the Fram strait including auxiliary sensors*. Norwegian Polar Institute. Retrieved from https://data.npolar.no/dataset/493ea7ad-a9b3-4dbd-8111-2bec154fae29

Dodd, P. A., Gonçalves-Araujo, R., Granskog, M. A., Jensen, A. D. B., Kern, Y., Lin, G., et al. (2022). *CTD profiles from NPI cruise FS2021 to the Fram strait including auxiliary sensors*. Norwegian Polar Institute. Retrieved from https://data.npolar.no/dataset/17b6bec5-a863-4713-be88-c13f83b934b2

Fahrbach, E., Meincke, J., Østerhus, S., Rohardt, G., Schauer, U., Tverberg, V., & Verduin, J. (2001). Direct measurements of volume transports through Fram Strait. *Polar Research*, *20*(2), 217–224. https://doi.org/10.1111/j.1751-8369.2001.tb00059.x

Foukal, N. P., Gelderloos, R., & Pickart, R. S. (2020). A continuous pathway for fresh water along the East Greenland shelf. *Science Advances*, *6*(43), eabc4254. https://doi.org/10.1126/sciadv.abc4254

Håvik, L., Pickart, R. S., Våge, K., Torres, D., Thurnherr, A. M., Beszczynska-Möller, A., et al. (2017). Evolution of the East Greenland current from Fram Strait to Denmark strait: Synoptic measurements from summer 2012. *Journal of Geophysical Research: Oceans*, *122*(3), 1974–1994. https://doi.org/10.1002/2016JC012228

Håvik, L., & Våge, K. (2018). Wind-driven coastal upwelling and downwelling in the shelfbreak east Greenland current. *Journal of Geophysical Research: Oceans*, *123*(9), 6106–6115. https://doi.org/10.1029/2018JC014273

Hersbach, H., Bell, B., Berrisford, P., Hirahara, S., Horányi, A., Muñoz-Sabater, J., et al. (2020). The ERA5 global reanalysis. *Quarterly Journal of the Royal Meteorological Society*, *146*(730), 1999–2049. https://doi.org/10.1002/qj.3803

Holfort, J., & Meincke, J. (2005). Time series of freshwater-transport on the East Greenland shelf at 74N. *Meteorologische Zeitschrift*, *14*(6), 703–710. https://doi.org/10.1127/0941-2948/2005/0079

Karpouzoglou, T., & de Steur, L. (2021). *Fram strait gridded monthly mean velocity and salinity and time-series of freshwater transport, freshwater content, volume transport and salt transport since 2003*. Norwegian Polar Institute. https://doi.org/10.21334/npolar.2021.049178d8

Karpouzoglou, T., de Steur, L., Smedsrud, L. H., & Sumata, H. (2022). Observed changes in the Arctic freshwater outflow in Fram Strait. *Journal of Geophysical Research: Oceans*, *127*(3), e2021JC018122. https://doi.org/10.1029/2021JC018122

Le Bras, I., Straneo, F., Muilwijk, M., Smedsrud, L. H., Li, F., Lozier, M. S., & Holliday, N. P. (2021). How much Arctic fresh water participates in the subpolar overturning circulation? *Journal of Physical Oceanography*, *51*(3), 955–973. https://doi.org/10.1175/JPO-D-20-0240.1

Müller, F. L., Dettmering, D., Wekerle, C., Schwatke, C., Bosch, W., & Seitz, F. (2019). Geostrophic currents in the northern Nordic seas - a combined dataset of multi-mission satellite altimetry and ocean modeling (data) [Dataset]. PANGAEA. (Supplement to: Müller, Felix L; Dettmering, Denise; Wekerle, Claudia; Schwatke, Christian; Passaro, Marcello; Bosch, Wolfgang; Seitz, Florian (2019): Geostrophic currents in the northern Nordic Seas from a combination of multi-mission satellite altimetry and ocean modeling. Earth System Science Data, 11(4), 1765-1781). https://doi.org/10.1594/PANGAEA.900691

Münchow, A., Schaffer, J., & Kanzow, T. (2020). Ocean circulation connecting Fram Strait to glaciers off Northeast Greenland: Mean flows, topographic Rossby waves, and their forcing. *Journal of Physical Oceanography*, *50*(2), 509–530. https://doi.org/10.1175/JPO-D-19-0085.1

Rabe, B., Dodd, P. A., Hansen, E., Falck, E., Schauer, U., Mackensen, A., et al. (2013). Liquid export of Arctic freshwater components through the Fram Strait 1998-2011. *Ocean Science*, *9*(1), 91–109. https://doi.org/10.5194/os-9-91-2013

Rigor, I. G., Wallace, J. M., & Colony, R. L. (2002). Response of sea ice to the Arctic oscillation. *Journal of Climate*, *15*(18), 2648–2663. https://doi.org/10.1175/1520-0442(2002)015⟨2648:ROSITT⟩2.0.CO;2

Rose, S. K., Andersen, O. B., Passaro, M., Ludwigsen, C. A., & Schwatke, C. (2019a). Arctic Ocean sea level record from the complete radar altimetry era: 1991–2018. *Remote Sensing*, *11*(14), 1672. https://doi.org/10.3390/rs11141672

Rose, S. K., Andersen, O. B., Passaro, M., Ludwigsen, C. A., & Schwatke, C. (2019b). DTU's Arctic Ocean sea level product [Dataset]. DTU. https://doi.org/10.11583/DTU.15124530

Rudels, B., Björk, G., Nilsson, J., Winsor, P., Lake, I., & Nohr, C. (2005). The interaction between waters from the Arctic Ocean and the Nordic seas north of Fram Strait and along the East Greenland current: Results from the Arctic Ocean-02 oden expedition. *Journal of Marine Systems*, *55*(1), 1–30. https://doi.org/10.1016/j.jmarsys.2004.06.008

Schaffer, J., von Appen, W.-J., Dodd, P. A., Hofstede, C., Mayer, C., de Steur, L., & Kanzow, T. (2017). Warm water pathways toward Nioghalvfjerdsfjorden glacier, Northeast Greenland. *Journal of Geophysical Research: Oceans*, *122*(5), 4004–4020. https://doi.org/10.1002/2016JC012462

Schauer, U., & Losch, M. (2019). "Freshwater" in the ocean is not a useful parameter in climate research. *Journal of Physical Oceanography*, *49*(9), 2309–2321. https://doi.org/10.1175/JPO-D-19-0102.1

Stommel, H. (1961). Thermohaline convection with two stable regimes of flow. *Tellus*, *13*(2), 224–230. https://doi.org/10.3402/tellusa.v13i2.9491

Topp, R., & Johnson, M. (1997). Winter intensification and water mass evolution from yearlong current meters in the Northeast Water Polynya. *Journal of Marine Systems*, *10*(1), 157–173. https://doi.org/10.1016/S0924-7963(96)00083-8

Tsubouchi, T., Bacon, S., Aksenov, Y., Garabato, A. C. N., Beszczynska-Möller, A., Hansen, E., et al. (2018). The Arctic Ocean seasonal cycles of heat and freshwater fluxes: Observation-based inverse estimates. *Journal of Physical Oceanography*, *48*(9), 2029–2055. https://doi.org/10.1175/jpo-d-17-0239.1

References From the Supporting Information

Müller, F. L., Dettmering, D., Wekerle, C., Schwatke, C., Passaro, M., Bosch, W., & Seitz, F. (2019). Geostrophic currents in the northern Nordic Seas from a combination of multi-mission satellite altimetry and ocean modeling. *Earth System Science Data*, *11*(4), 1765–1781. https://doi.org/10.5194/essd-11-1765-2019

Padman, L., & Erofeeva, S. (2004). A barotropic inverse tidal model for the Arctic Ocean. *Geophysical Research Letters*, *31*(2). https://doi.org/10.1029/2003GL019003